A Fourier series based generalized yield surface description for the efficient modelling of orthotropic sheet metals

Author(s):
Raemy, Christian; Manopulo, Niko; Hora, Pavel

Publication date:
2017

Permanent link:
https://doi.org/10.3929/ethz-b-000188528

Originally published in:
Journal of Physics: Conference Series 896(1), https://doi.org/10.1088/1742-6596/896/1/012016

A Fourier series based generalized yield surface description for the efficient modelling of orthotropic sheet metals

IOP Conf. Series: Journal of Physics: Conf. Series **896** (2017) 012016 doi:10.1088/1742-6596/896/1/012016

A Fourier series based generalized yield surface description for the efficient modelling of orthotropic sheet metals

C Raemy, N Manopulo and P Hora

Institute of Virtual Manufacturing, ETH Zurich, Tannenstrasse 3, 8092 Zurich, Switzerland

E-mail: manopulo@ivp.mavt.ethz.ch

Abstract. In the current state of the art, there exist a large number of different yield surface descriptions, which are well established in modelling particular types of materials. The success of a particular model is primarily related to its ability of accurately representing the material behaviour based on a limited number of experiments. In the present work, instead of defining a particular mathematical formulation, a generic yield surface is proposed based on a 2D Fourier series. Yield surfaces of increasing complexity can be effectively generated by increasing the number of terms in the series. The particular properties of the modelled materials are not derived from a predefined formulation, but enforced as a set of constraints. It is shown that both symmetric and asymmetric yield loci can be easily constructed using this approach. Furthermore the accuracy and computational efficiency of the proposed model is discussed in comparison to well established yield surface functions, using deep drawing simulations.

1. Introduction

The accuracy of metal forming simulations relies among others on the ability of the constitutive model to reproduce the material behaviour and the quality of the corresponding experimental input data. Since the middle of the 20th century, numerous anisotropic yield criteria have been proposed with continuously increasing complexity, e.g.[1, 2, 3, 4, 5]. Most models make use of one or more linear transformations of the stress tensor and functions of the eigenvalues or invariants thereof. It has become evident that those criteria might be well-suited for a specific kind of material, but fall behind when applied to another. At worst, they cannot capture a specific behaviour at all e.g. most models cannot describe tension-compression asymmetry which is exhibited by some materials.

Furthermore, to map complex anisotropy, additional degrees of freedom have to be added to the criteria. This is mostly accomplished by the introduction of additional linear transformations which in turn induce additional eigenvalue computations, increasing calculation time. As an alternative, it was proposed to drop the constraint of associated flow, thus using separate functions for determining flow stresses and flow directions [6]. The discussion about the physical motivation of this approach is still ongoing in the scientific community.

We propose a formally compact model on the basis of a two-dimensional Fourier series which makes use of an associated flow rule, overcoming the mentioned limitations. By simply adding more coefficients to the series, virtually any shape of the flow surface can be realized

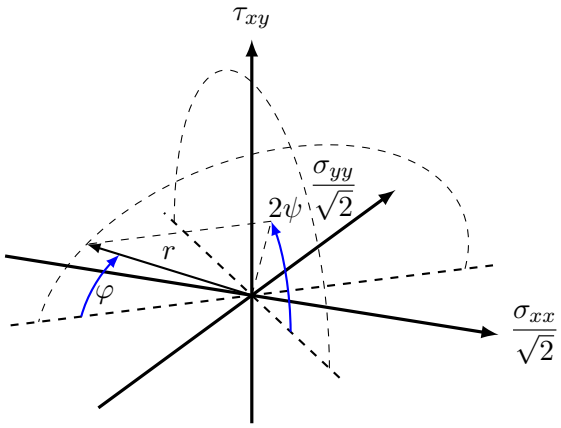

Figure 1. Embedding of the spherical coordinates in space of plane stress states

without significantly increasing the computational costs. It is applicable for both symmetric and asymmetric materials; even non-orthotropic behaviour could be treated.

2. Proposed model

2.1. Definition

The space of plane stress states is typically parametrized by Cartesian coordinates $\{\sigma_{xx}, \sigma_{yy}, \tau_{xy}\}$ and flow criteria are homogeneous functions of first order of these components. To make use of a Fourier series, a periodic parametrization is needed, which is readily found in spherical coordinates $\{r, \varphi, \psi\}$, where r represents the radius, φ is the polar and ψ the azimuthal angle. In order to exploit the natural symmetries of the flow surfaces it is not recommended to embed these coordinates in the canonical way, where the north pole points in positive τ_{xy} direction and the azimuthal angle is measured from positive σ_{xx} direction. Instead the embedding shown in Figure 1 is used, where the north pole points to balanced biaxial compression and the azimuthal angle is measured from the straight line $\{\sigma_{xx} = -\sigma_{yy}, \tau_{xy} = 0\}$. Note that the normal stresses are scaled by a factor of $1/\sqrt{2}$ and the azimuthal angle is expressed by 2ψ. In that way, uniaxial tension at an arbitrary angle θ to rolling direction can be parametrized with constant values of r and φ, while $\psi = \theta$. This will be demonstrated below. The mapping between the parametrizations is given by

$$r = \sqrt{\frac{\sigma_{xx}^2}{2} + \frac{\sigma_{yy}^2}{2} + \tau_{xy}^2} \tag{1a}$$

$$\varphi = \arccos\left(-\frac{\sigma_{xx} + \sigma_{yy}}{2r}\right) \tag{1b}$$

$$\psi = \frac{1}{2}\operatorname{arctan2}\Big(2\tau_{xy}, (\sigma_{xx} - \sigma_{yy})\Big). \tag{1c}$$

A two dimensional Fourier series of φ and ψ is an infinite weighted sum

$$\begin{aligned} f(\varphi,\psi) = &\sum_{m=0}^{\infty}\sum_{n=0}^{\infty} a_{m,n}\cos(m\varphi)\cos(n\psi) \quad + \sum_{m=0}^{\infty}\sum_{n=1}^{\infty} b_{m,n}\cos(m\varphi)\sin(n\psi) \\ &+ \sum_{m=1}^{\infty}\sum_{n=0}^{\infty} c_{m,n}\sin(m\varphi)\cos(n\psi) \quad + \sum_{m=1}^{\infty}\sum_{n=1}^{\infty} d_{m,n}\sin(m\varphi)\sin(n\psi)\,. \end{aligned} \tag{2}$$

With the definitions (1) and (2), an equivalent stress of the formally compact form

$$\bar{\sigma}(r,\varphi,\psi) = r\sqrt[q]{f(\varphi,\psi)} \tag{3}$$

is proposed, which is called "FAY" hereinafter (Fourier Anisotropic Yield).

It can be shown that von Mises' criterion reads in this parametrization as

$$\bar{\sigma}_{\mathrm{vM}}^2 = r^2 \cdot \Big(2 - \cos(2\varphi)\Big). \tag{4}$$

and the equivalent to Hosford's isotropic flow function [2] (in terms of principal stresses)

$$\bar{\sigma}_{\mathrm{Hosf}}^q = \frac{|\sigma_1|^q + |\sigma_2|^q + |\sigma_1 - \sigma_2|^q}{2} \tag{5}$$

is e.g. for $q = 6$

$$\bar{\sigma}_{\mathrm{Hosf}}^6 = r^6 \left(\frac{25}{2} - 15\cos(2\varphi) + \frac{9}{2}\cos(4\varphi) - \cos(6\varphi)\right). \tag{6}$$

Note that these isotropic criteria do not depend on ψ, which is related to the orientation of the sheet. This does not hold for Hill's plane stress function [1]

$$\bar{\sigma}_{\mathrm{Hill}}^2 = (G+H)\,\sigma_{xx}^2 - 2H\sigma_{xx}\sigma_{yy} + (H+F)\,\sigma_{yy}^2 + 2N\tau_{xy}^2, \tag{7}$$

which can be expressed equivalently using the coefficients

$$\begin{aligned} a_{0,0} &= \frac{3F+3G+4H+2N}{4} & a_{0,4} &= \frac{F+G+4H-2N}{4} \\ a_{2,0} &= \frac{F+G-4H-2N}{4} & a_{2,4} &= \frac{-F-G-4H+2N}{4} \\ c_{2,2} &= -F+G & q &= 2. \end{aligned} \tag{8}$$

Care must be taken when choosing the coefficients in order to respect physical constraints:

- The yield surface must be closed and – for an orthotropic material – symmetric with respect to the plane $\tau_{xy} = 0$. This implies that only cosine terms of even multiples of ψ must occur

$$a_{m,n} = c_{m,n} = 0 \quad \text{if } n \text{ is odd} \tag{9a}$$
$$b_{m,n} = d_{m,n} = 0 \quad \forall\,\{m,n\}\,. \tag{9b}$$

- Tension-compression symmetry requieres $f(\varphi,\psi) \equiv f\left(\pi-\varphi, \frac{\pi}{2}-\psi\right)$, hence

$$a_{m,n} = 0 \quad \text{if } \{m \text{ is even and } n/2 \text{ is odd}\} \text{ or } \{m \text{ is odd and } n/2 \text{ is even}\} \tag{10a}$$
$$c_{m,n} = 0 \quad \text{if } \{m \text{ is even and } n/2 \text{ is even}\} \text{ or } \{m \text{ is odd and } n/2 \text{ is odd}\}\,. \tag{10b}$$

- To keep the surface smooth where the parametrization is singular (i.e. biaxial tension and compression)

$$\partial f/\partial\psi \equiv 0 \quad \text{at } \varphi = \{0,\pi\}\,, \forall\psi \tag{11a}$$
$$\partial f/\partial\varphi = 0 \quad \text{at } \varphi = \{0,\pi\}\,, \psi = \pi/4 \tag{11b}$$

  is required.

Clearly, the mentioned examples fulfill all of these constraints.

2.2. Properties

For uniaxial tensile (ut) stress with magnitude σ acting at an angle θ to rolling direction, the components of the stress tensor in the system of orthotropy read as

$$\boldsymbol{\sigma}^{\mathrm{ut}} = \frac{1}{2}\begin{pmatrix} 1+\cos(2\theta) & \sin(2\theta) \\ \sin(2\theta) & 1-\cos(2\theta) \end{pmatrix}\sigma. \tag{12}$$

Inserting this into definition (1), one deduces that

$$r^{\mathrm{ut}}(\theta) = \frac{\sqrt{2}}{2}\sigma \qquad \varphi^{\mathrm{ut}}(\theta) = \frac{3\pi}{4} \qquad \psi^{\mathrm{ut}}(\theta) = \theta, \tag{13}$$

i.e. two coordinates are constant for this stress state, which simplifies the fitting procedure.

The derivatives of the flow function (3) with respect to the stress components can be expressed as

$$\frac{\partial\bar{\sigma}}{\partial\sigma_{xx}} = P\left[qf\frac{\sin(\varphi)\cos(2\psi)-\cos(\varphi)}{2} + \frac{\partial f}{\partial\varphi}\frac{\cos(\varphi)\cos(2\psi)+\sin(\varphi)}{2} - \frac{\partial f}{\partial\psi}\frac{\sin(2\psi)}{4\sin(\varphi)}\right] \tag{14a}$$

$$\frac{\partial\bar{\sigma}}{\partial\sigma_{yy}} = P\left[qf\frac{-\sin(\varphi)\cos(2\psi)-\cos(\varphi)}{2} + \frac{\partial f}{\partial\varphi}\frac{-\cos(\varphi)\cos(2\psi)+\sin(\varphi)}{2} + \frac{\partial f}{\partial\psi}\frac{\sin(2\psi)}{4\sin(\varphi)}\right] \tag{14b}$$

$$\frac{\partial\bar{\sigma}}{\partial\tau_{xy}} = P\left[qf\sin(\varphi)\sin(2\psi) + \frac{\partial f}{\partial\varphi}\cos(\varphi)\sin(2\psi) + \frac{\partial f}{\partial\psi}\frac{\cos(2\psi)}{2\sin(\varphi)}\right], \tag{14c}$$

where $P = \frac{1}{q}\left(\frac{r}{\bar{\sigma}}\right)^{q-1}$. Using this result and an associated flow rule, the R-value for a uniaxial tensile test in θ-direction can be calculated by (the derivations are carried out in more detail in [7])

$$R(\theta) = -\frac{\partial f/\partial\varphi}{qf + \partial f/\partial\varphi}, \tag{15}$$

which has to be evaluated at $\varphi = \varphi^{\mathrm{ut}} = \frac{3\pi}{4}$ and $\psi = \psi^{\mathrm{ut}} = \theta$.

2.3. Calibration

To calibrate the model, a set of Fourier coefficients has to be found which deliver a convex surface (see below) while reproducing the experimental data and complying with the restrictions mentioned in paragraph 2.1. In the following, it is assumed that the material is symmetric and tensile tests in 3 directions have been carried out (in 0°, 45° and 90° to rolling direction); extension to more experiments is straightforward.

The basic idea of the procedure is to define one-dimensional "input series" which represent cuts through the two-dimensional series $f(\varphi,\psi)$ or its partial derivatives. The input series are obtained by the experimental data of uniaxial tensile tests. From the measured flow stresses, a three-component Fourier series

$$g(\theta) = g_0 + g_1\cos(2\theta) + g_2\cos(4\theta) \tag{16}$$

is calibrated, such that

$$g(0) = \left(\frac{\sqrt{2}\sigma_{\mathrm{ref}}}{\sigma_0}\right)^q \qquad g(\pi/4) = \left(\frac{\sqrt{2}\sigma_{\mathrm{ref}}}{\sigma_{45}}\right)^q \qquad g(\pi/2) = \left(\frac{\sqrt{2}\sigma_{\mathrm{ref}}}{\sigma_{90}}\right)^q. \tag{17}$$

Similarly, the measured R-values give a series

$$h(\theta) = h_0 + h_1 \cos(2\theta) + h_2 \cos(4\theta) \tag{18}$$

such that

$$h(0) = -q\frac{R_0}{R_0+1}g(0) \qquad h(\pi/4) = -q\frac{R_{45}}{R_{45}+1}g(\pi/4) \qquad h(\pi/2) = -q\frac{R_{90}}{R_{90}+1}g(\pi/2). \tag{19}$$

Forcing

$$f(\varphi = \varphi^{\mathrm{ut}}, \psi = \theta) = g(\theta), \qquad \frac{\partial f(\varphi = \varphi^{\mathrm{ut}}, \psi = \theta)}{\partial \varphi} = h(\theta) \qquad \forall\theta \tag{20}$$

now ensures that the proposes model exactly reproduces the measured values while staying smooth. Additional constraints on f can be derived in order to force correct values of biaxial flow stress, biaxial "R-value" (see [7]) and plane-strain points.

Uniqueness of the solution of the stress return mapping requires the flow surface to be strictly convex. To the knowledge of the authors, this is not easy to achieve analytically. Instead, the examination is carried out numerically by calculating the Gaussian curvature

$$K(\varphi, \psi) = \frac{LN - M^2}{EG - F^2} \tag{21}$$

of the surface from its explicit parametrization

$$\boldsymbol{x}(\varphi, \psi) = \frac{\sigma_{\mathrm{ref}}}{\sqrt[q]{f(\varphi, \psi)}} \begin{pmatrix} \sin(\varphi)\cos(2\psi) - \cos(\varphi) \\ -\sin(\varphi)\cos(2\psi) - \cos(\varphi) \\ \sin(\varphi)\sin(2\psi) \end{pmatrix}. \tag{22}$$

E, F, G, L, M, N are the components of the first and second fundamental forms

$$\begin{pmatrix} E & F \\ F & G \end{pmatrix} = \begin{pmatrix} \boldsymbol{x}_{,\varphi} \cdot \boldsymbol{x}_{,\varphi} & \boldsymbol{x}_{,\varphi} \cdot \boldsymbol{x}_{,\psi} \\ \boldsymbol{x}_{,\psi} \cdot \boldsymbol{x}_{,\varphi} & \boldsymbol{x}_{,\psi} \cdot \boldsymbol{x}_{,\psi,} \end{pmatrix}, \quad \begin{pmatrix} L & M \\ M & N \end{pmatrix} = \begin{pmatrix} \boldsymbol{\nu} \cdot \boldsymbol{x}_{,\varphi\varphi} & \boldsymbol{\nu} \cdot \boldsymbol{x}_{,\varphi\psi} \\ \boldsymbol{\nu} \cdot \boldsymbol{x}_{,\psi\varphi} & \boldsymbol{\nu} \cdot \boldsymbol{x}_{,\psi\psi} \end{pmatrix}, \quad \boldsymbol{\nu} = \frac{\boldsymbol{x}_{,\varphi} \times \boldsymbol{x}_{,\psi}}{\|\boldsymbol{x}_{,\varphi} \times \boldsymbol{x}_{,\psi}\|}. \tag{23}$$

Hereby, a subscript preceded by a comma denotes a partial derivative and $\boldsymbol{\nu}$ is the normalized outward normal on the flow surface, which is obtained by the cross product of two tangential vectors. The curvature is calculated on a densely populated sample of the parameter space $\{\varphi \in [0, \pi], \psi \in [0, \pi/2]\}$. If all i values are positive, the surface is assumed to be strictly convex. Therefore, a maximin optimization

$$\max_{\{a_{m,n}, c_{m,n}\}} \left[\min_i \big(K(\varphi_i, \psi_i) \big) \right] \tag{24}$$

subject to the mentioned constraints is carried out in order to maximize the lowest Gaussian curvature. By adding non-zero coefficients $a_{m,n}, c_{m,n}$ to f, finding a positive solution is possible in general.

3. Examples of application

The model was calibrated for two materials showing a complex behaviour (oscillation of uniaxial flow stresses and R-values). Park and Chung [8] used these examples to demonstrate the advantages of a non-associated flow rule. They calibrated the model yld2000-2d [4] in three different ways:

- Using the uniaxial data in rolling, diagonal and transverse direction as well the biaxial flow stress and flow direction to get the standard associated model (labelled "associated" in the legend)
- Using only the flow stresses to get a flow surface for the non-associated flow rule (labelled "yield")
- Using only the R-values to get a flow potential for the non-associated flow rule (labelled "potential")

All experimental data and model parameters can be found in the mentioned publication. [1]

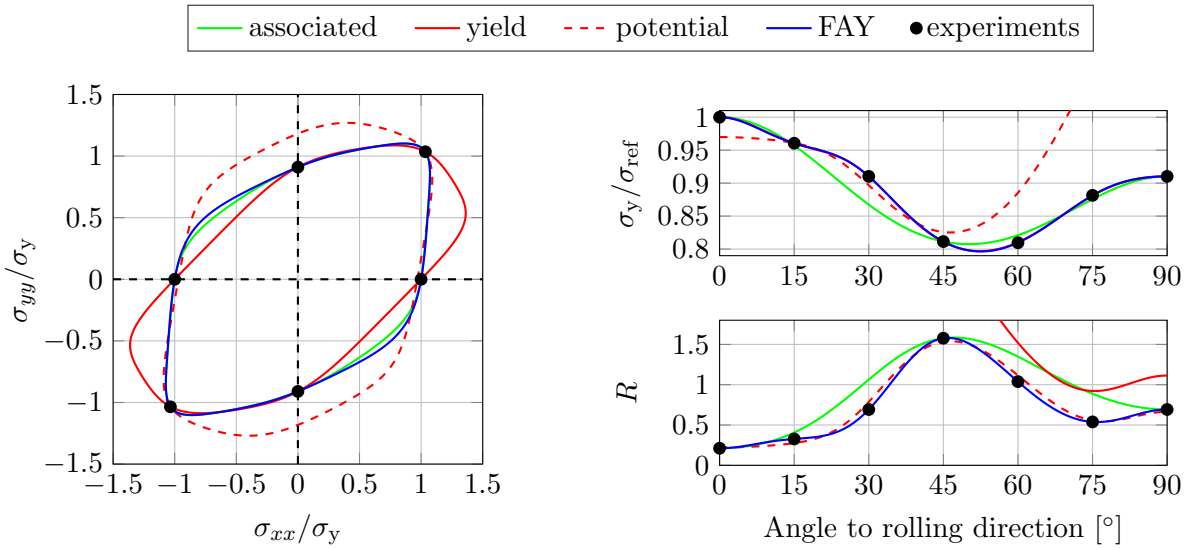

Figure 2. Predicted yield locus, uni-axial flow stresses and R-values for AA2090-T3. Experimental data and parameters for yld2000-2d models taken from [8]

For both materials it can be observed that the associated model captures the data points which were used for the calibration, but also give a good estimate for the non-considered flow stresses and R-values (Figures 2 and 3). On the other hand the non-associated yield surfaces capture all flow stress, but predict unrealistic R-values (clearly, they are not needed in the case of non-associated flow). Additionally for the AA2090-T3 material, an unnaturally high strength is predicted in the plane-strain region, while the region of pure shear suffers from softening compared to the associated yield locus.

The non-associated flow-potentials can reproduce the experimental R-values quite accurately, though not exactly. For the AA5042 material, the corresponding locus shows rather sharp edges due to the high exponent ($a = 14$) chosen by the authors.

The proposed FAY model is able to combine the advantages of all three models calibrated by Park and Chung: The predicted yield loci are smooth and almost identical to those of the associated models. All uniaxial flow stress are predicted exactly, the same holds for the R-values except for R_{15} of the AA5042 material (forcing the model to capture this value resulted in a non-convex yield surface).

4. Comparative study

Park and Chung [8] implemented their models into a commercial FE code in order to simulate a cup drawing test. For the present study yld2000-2d (associated and non-associated) and FAY

[1] The plain strain point is an important feature of every yield surface and should ideally be measured [9]. As this quantity was not given in the publication, the yld2000-2d prediction has been used to calibrate FAY.

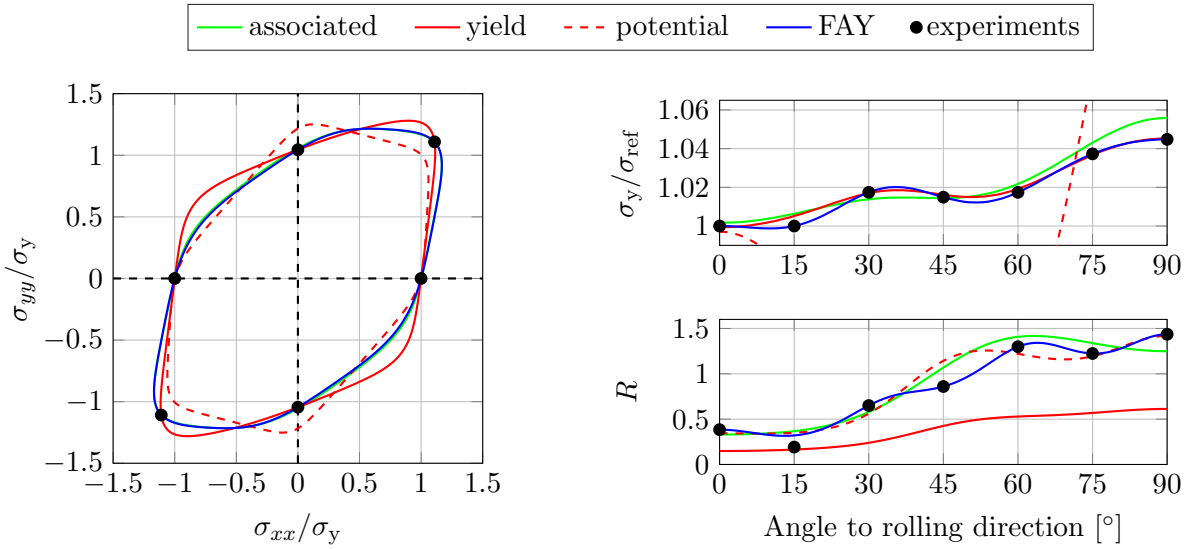

Figure 3. Predicted yield locus, uni-axial flow stresses and R-values for AA5042. Experimental data and parameters for yld2000-2d models taken from [8].

were implemented for explicit LS-Dyna with closest point return mapping [10]. It was tried to built a numerical model close to the one used by Park and Chung, who used the height profile of the final cup to assess the accuracy of the models. The results of the present study are visualized in Figure 4.

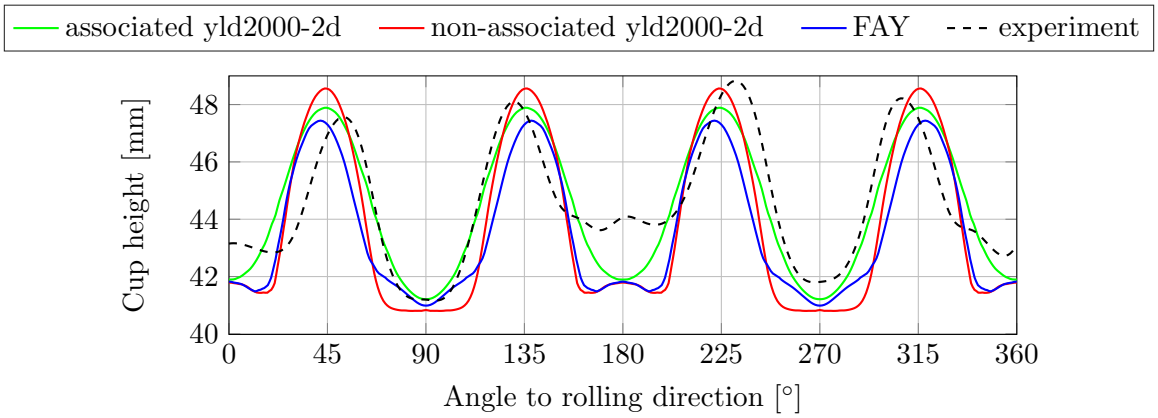

Figure 4. Predicted earing profile of AA2090-T3 cup. Experimental data and parameters for yld2000-2d models taken from [8].

It can be observed that the associated yld2000-2d model delivers a very smooth result, reflecting the smoothly predicted R-values. The non-associated yld2000-2d model is able to predict also the ear at 0° and 180°, which is not the case for the associated yld2000-2d formulation. On the other hand, the overall draw-in at this position is overestimated, as it is the case with all presented models. FAY lies between the two yld2000-2d functions, predicting the small ears at 0° and 180° like non-associated yld2000-2d but giving a rather sharp ear at 90° and 270° like associated yld2000-2d.

In terms of total computational costs the models are almost equivalent. Again FAY lies between the associated and non-associated yld2000-2d models, as Figure 5 illustrates.

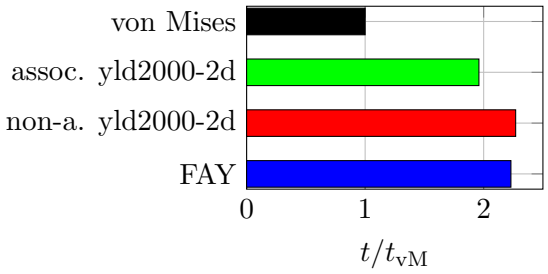

Figure 5. CPU time of cup drawing simulation, normalized with respect to built-in von Mises.

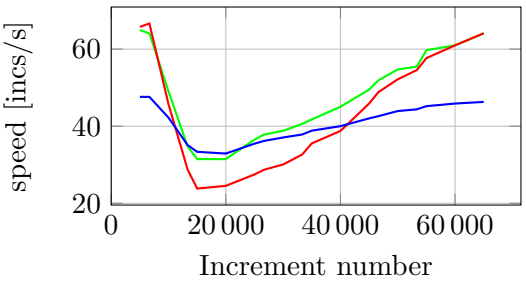

Figure 6. Evolution of calculation speed during cup drawing simulation.

The comparatively small computational advantage of FAY lies in the fact that a significant portion of the computation remains elastic in the considered model. In fact, as it can be seen in Figure 6, the non-associated yld2000-2d is faster than FAY in the initial and final steps of the computation where elastic deformation is dominant. FAY is at clear advantage in-between where the geometry is almost fully plastified. This is because the yield stress computation is slightly more expensive in FAY than in yld2000-2d, but the first and second derivatives are much faster than with the latter.

5. Conclusions

A formally simple yield criterion for sheet metal was introduced. As it is based on a two-dimensional Fourier series, its complexity can be controlled by the number of considered coefficients. Although adding coefficients to the series allows for capturing more experimental data, the formal structure of the model and its derivatives remains unaltered and calculation time increases only insignificantly. The model was calibrated for two materials with rather complex behaviour. It was shown that – although an associated flow rule was used – flow stresses and R-values could be reproduced even more accurately than by the use of a high-order flow function combined with a non-associated flow rule.

References

[1] Hill R 1948 A theory of the yielding and plastic flow of anisotropic metals *Proc. of the Royal Society of London* A **193** 281–97
[2] Hosford W F 1972 A generalized isotropic yield criterion *J. of Applied Mechanics* **39** 607–9
[3] Barlat F and Lian K 1989 Plastic behavior and stretchability of sheet metals. Part I: A yield function for orthotropic sheets under plane stress conditions *Int. J. of Plasticity* **5** 5166
[4] Barlat F, Brem J C, Yoon J W, Chung K, Dick R E, Lege D J, Pourboghrat F, Choi S. H. and Chu E 2003 Plane stress yield function for aluminum alloy sheets part 1: theory *Int. J. of Plasticity* **19** 1297–319
[5] Bron F and Besson J 2004 A yield function for anisotropic materials application to aluminum alloys *Int. J. of Plasticity* **20** 937–963
[6] Stoughton T B 2002 A non-associated flow rule for sheet metal forming *Int. J. of Plasticity* **18** 687–714
[7] Raemy C, Manopulo N and Hora P, 2017 On the modelling of plastic anisotropy, asymmetry and directional hardening of commercially pure titanium: A planar Fourier series based approach *Int. J. of Plasticity* Article in press
[8] Park T and Chung K 2012 Non-associated flow rule with symmetric stiffness modulus for isotropic-kinematic hardening and its application for earing in circular cup drawing *Int. J. of Solids and Structures* **49** 3582–93
[9] An Y G, Vegter H and Elliott L, 2004 A novel and simple method for the measurement of plane strain work hardening *J. of Materials Processing Technology* **155–156** 1616–22
[10] Simo J C and Hughes T J R 1998 *Computational Inelasticity* (New York: Springer) pp 143–145